1521-0111/83/5/1007–1019$25.00
MOLECULAR PHARMACOLOGY

http://dx.doi.org/10.1124/mol.112.084319
Mol Pharmacol 83:1007–1019, May 2013

Sensory Nerve Terminal Mitochondrial Dysfunction Activates Airway Sensory Nerves via Transient Receptor Potential (TRP) Channels

Lika Nesuashvili, Stephen H. Hadley, Parmvir K. Bahia, and Thomas E. Taylor-Clark

Department of Molecular Pharmacology and Physiology, College of Medicine, University of South Florida, Tampa, Florida

Received December 7, 2012; accepted February 25, 2013

ABSTRACT

Mitochondrial dysfunction and subsequent oxidative stress has been reported for a variety of cell types in inflammatory diseases. Given the abundance of mitochondria at the peripheral terminals of sensory nerves and the sensitivity of transient receptor potential (TRP) ankyrin 1 (A1) and TRP vanilloid 1 (V1) to reactive oxygen species (ROS) and their downstream products of lipid peroxidation, we investigated the effect of nerve terminal mitochondrial dysfunction on airway sensory nerve excitability. Here we show that mitochondrial dysfunction evoked by acute treatment with antimycin A (mitochondrial complex III Q_i site inhibitor) preferentially activated TRPA1-expressing "nociceptor-like" mouse bronchopulmonary C-fibers. Action potential discharge was reduced by the TRPA1 antagonist HC-030031. Inhibition of TRPV1 further reduced C-fiber activation. In mouse dissociated vagal neurons, antimycin A induced Ca^{2+} influx that was significantly reduced by pharmacological inhibition or genetic knockout of either TRPA1 or TRPV1. Inhibition of both TRPA1 and TRPV1 was required to abolish antimycin A-induced Ca^{2+} influx in vagal neurons. Using an HEK293 cell expression system, antimycin A induced concentration-dependent activation of both hTRPA1 and hTRPV1 but failed to activate nontransfected cells. Myxothiazol (complex III Q_o site inhibitor) inhibited antimycin A-induced TRPA1 activation, as did the reducing agent dithiothreitol. Scavenging of both superoxide and hydrogen peroxide inhibited TRPA1 activation following mitochondrial modulation. In conclusion, we present evidence that acute mitochondrial dysfunction activates airway sensory nerves preferentially via TRPA1 through the actions of mitochondrially-derived ROS. This represents a novel mechanism by which inflammation may be transduced into nociceptive electrical signaling.

Introduction

There is growing evidence that mitochondrial dysfunction contributes to the complex mechanisms of multiple diseases. In addition to diseases of inherited and spontaneous mutations in nuclear or mitochondrial DNA (leading to altered mitochondrial protein expression) (Copeland, 2008), increased mitochondrial reactive oxygen species (ROS) production is thought to contribute to chronic inflammatory disease states such as type II diabetes mellitus, cardiovascular disease, asthma, and irritable bowel syndrome (Hall and Wiley, 1998; Rocha et al., 2010; Reddy, 2011; Chowdhury et al., 2013).

Mitochondria are present in the vast majority of nucleated cells including sensory nerves. ATP production is coupled to oxygen reduction by electron transport chain (ETC) proteins of the mitochondrial inner membrane. During normal physiologic conditions approximately 2% of oxygen undergoes incomplete reduction and produces the ROS superoxide. Inefficiencies of ETC proteins in complexes I and III lead to excess superoxide production and, through a series of reactions, the downstream formation of ROS and lipid peroxidation products (e.g., 4-hydroxynonenal) (Karihtala and Soini, 2007). Although the mechanism of mitochondrial dysfunction in chronic inflammatory diseases is not well understood, numerous inflammatory signaling pathways increase mitochondrial ROS production either: 1) through the inhibition of complexes I or III [e.g., tumor necrosis factor α (Corda et al., 2001), neurotrophins via p75NTR (Pehar et al., 2007), and Toll-like receptors (West et al., 2011)]; or 2) through downregulation of mitochondrial antioxidant enzymes by microRNAs (Aroor et al., 2012) and transforming growth factor β (Michaeloudes et al., 2011).

In the respiratory system, mitochondrial dysfunction and oxidative stress has been described in airway epithelial and smooth muscle cells in asthma and chronic obstructive pulmonary disease (Rabinovich et al., 2007; Mabalirajan et al., 2008; Aguilera-Aguirre et al., 2009). The airways and lungs are densely innervated with vagal sensory nerves. Interestingly, the peripheral terminals of these nerves, which

This work was supported by the National Institutes of Health [Grant R00HL088520].
dx.doi.org/10.1124/mol.112.084319.

ABBREVIATIONS: Antimycin A, (2{R},3{S},6{S},7{R},8{R})-3-[(3-formamido-2-hydroxybenzoyl)amino]-8-hexyl-2,6-dimethyl-4,9-dioxo-1,5-dioxonan-7-yl 3-methylbutanoate; AITC, allyl isothiocyanate; cinnamaldehyde, (2*E*)-3-phenylprop-2-enal; DTNB, 5,5′-dithiobis-(2-nitrobenzoic acid); DTT, dithiothrietol; ETC, electron transport chain; FBS, fetal bovine serum; glutathione, (2*S*)-2-amino-4-{[(1*R*)-1[(carboxymethyl)carbamoyl]-2-sulfanylethyl]carbamoyl}butanoic acid; HEK293, human embryonic kidney 293 cells; I-RTX, 5′-iodoresiniferatoxin; myxothiazol, 7-{2′-[(1S,2E,4E)-1,6-dimethyl-2,4-heptadienyl][2,4'-bithiazol]-4-yl}-3,5-dimethoxy-4-methyl-(2E,4R,5S,6E)-2,6-heptadienamide; MnTMPyP, manganese(III) tetrakis(1-methyl-4-pyridyl)porphyrin; NTB, 2-nitro-5-thiobenzoate; ROS, reactive oxygen species; TRPA1, transient receptor potential ankyrin 1; TRPV1, transient receptor potential vanilloid 1.

innervate the submucosal and epithelial layers of the airways, contain a high density of mitochondria (Hung et al., 1973; von During and Andres, 1988). The vast majority of airway sensory nerves are "nociceptive," i.e., they serve to protect the airways through the initiation of reflexes (cough, hypersecretion, bronchospasm) and sensations (dyspnea, itch, urge to cough) (Carr and Undem, 2003). As such there is considerable interest in understanding the mechanisms through which inflammation and other noxious stimuli activate these nerves and induce debilitating morbidity. Airway nociceptive nerves selectively express ion channels such as transient receptor potential vanilloid 1 (TRPV1) (Kollarik et al., 2003) and transient receptor potential ankyrin 1 (TRPA1) (Nassenstein et al., 2008) that are activated by inflammatory mediators, oxidative stress, and downstream products of lipid peroxidation (Patapoutian et al., 2009). Previous studies have shown that activation of TRPV1 or TRPA1 leads to airway nociceptor-induced reflexes and thus produces symptoms similar to airway diseases (Forsberg et al., 1988; Carr and Undem, 2003; Andre et al., 2008). Based on the anatomic colocalization of mitochondria and TRP channels in peripheral nerve terminals, we propose that sensory nerve terminal mitochondrial modulation is linked to sensory nerve activation. Here we show that acute mitochondrial modulation activates airway vagal nociceptors predominantly through the gating of TRPA1 channels.

Materials and Methods

All experiments were approved by the University of South Florida Institutional Animal Care and Use Committee.

Dissociation of Mouse Vagal Ganglia. Male mice were killed by CO_2 asphyxiation followed by exsanguination. Vagal ganglia were immediately isolated and enzymatically dissociated from wild-type C57BL/6J, TRPA1$^{-/-}$, and TRPV1$^{-/-}$ mice (The Jackson Laboratory, Bar Harbor, ME), using previously described methods (Taylor-Clark et al., 2008a). Isolated neurons were plated onto poly-D-lysine and laminin-coated coverslips, incubated at 37°C in L-15 [supplemented with 10% fetal bovine serum (FBS)], and used within 24 hours.

Knockout Mice. Male TRPA1$^{+/-}$ (The Jackson Laboratory: B6; 129P-Trpa1tm1Kykw/J) were mated with female TRPA1$^{-/-}$. Male TRPV1$^{-/-}$ (The Jackson Laboratory: B6.129X1-Trpv1tm1Jul/J) were mated with female TRPV1$^{-/-}$. Homozygous knockout offspring used for the experiments were determined by genotyping.

Bronchopulmonary C-Fiber Extracellular Recordings. Male mice were killed by CO_2 asphyxiation followed by exsanguination. The innervated isolated lung preparation was prepared as previously described (Taylor-Clark et al., 2008a, 2009). Briefly, the airways and lungs with their intact extrinsic innervation (vagus nerve including vagal ganglia) were taken and placed in a dissecting dish containing Krebs bicarbonate buffer solution composed of (mM): 118 NaCl, 5.4 KCl, 1.0 NaH_2PO_4, 1.2 $MgSO_4$, 1.9 $CaCl_2$, 25.0 $NaHCO_3$, and 11.1 D-glucose, and equilibrated with 95% O_2 and 5% CO_2 (pH 7.3–7.4). Connective tissue was trimmed away leaving the trachea and lungs with their intact nerves. The airways were then pinned to the larger compartment of a custom-built two-compartment recording chamber that was lined with silicone elastomer (Sylgard). A vagal ganglion was pulled into the adjacent compartment of the chamber through a small hole and pinned. Both compartments were separately superfused with Krebs bicarbonate buffer (37°C). A sharp glass electrode was pulled by a Flaming Brown micropipette puller (P-87; Sutter Instruments, Novato, CA) and filled with 3 M NaCl solution. The electrode was inserted and placed near the cell bodies of vagal ganglion. The recorded action potentials were amplified (Microelectrode AC amplifier 1800; A-M Systems, Everett, WA), filtered (0.3 kHz of low cut-off and 1 kHz of high cut-off), and monitored on an oscilloscope (TDS1002B; Tektronix, Beaverton, OR). The scaled output from the amplifier was captured and analyzed by a Macintosh computer using NerveOfIt software (Phocis, Baltimore, MD). To measure conduction velocity, an electrical stimulation (S44; Grass Instruments, Quincy, MA) was applied to the center of the receptive field. The conduction velocity of the individual bronchopulmonary afferent was calculated by dividing the distance along the nerve pathway by the time delay between the shock artifact and the action potential evoked by electrical stimulation. Drugs were intratracheally applied as a 1-ml bolus over 10 seconds. Inhibition of TRPA1 (HC-030031, 30 μM) or TRPV1 [iodoresiniferatoxin (I-RTX), 1 μM] was achieved by addition of these inhibitors to the perfusion (10-minute pretreatment). The viability of a given bronchopulmonary C-fiber terminal was determined by action potential discharge to mechanical (von Frey fibers) and chemical stimuli [α,β methylene ATP ($P2X_{2/3}$ agonist, 30 μM)]. C-fibers were characterized for their expression of TRPA1 and TRPV1 channels by their response to selective TRPA1 agonists, cinnamaldehyde (300 μM) or allyl isothiocyanate (AITC, 300 μM), and to the selective TRPV1 agonist capsaicin (1 μM). Due to a lack of TRPV1 channels in bronchopulmonary C-fibers from TRPV1$^{-/-}$ mice, "nociceptive" status was assessed solely by conduction velocity and the response to TRPA1 agonists (Kollarik et al., 2003; Nassenstein et al., 2008). Due to the irreversible inhibition of complex III by antimycin (Potter and Reif, 1952; Slater, 1973; Turrens et al., 1985; Stowe and Camara, 2009), only one antimycin A treatment was used per preparation. Due to potential heterologous desensitization, capsaicin was only given at the end of each experiment. All excitatory chemical treatments were separated by wash of at least 15 minutes. Action potential discharge was quantified off-line and recorded in 1-second bins. A response was considered positive if the number of action potentials in any 1-second bin was twice the average background response. The background activity was usually either absent or less than 2 Hz. The peak frequency evoked by a stimulus was quantified as the maximum number of action potentials that occurred within any 1-second bin.

HEK293 Cell Culture. Wild-type nontransfected HEK293 cells (nt-HEK), stably expressing human TRPA1-HEK cells (hTRPA1-HEK) and stably expressing hTRPV1-HEK cells were previously obtained from GlaxoSmithKline. These HEK cells were cultured as previously described (Taylor-Clark et al., 2008a). Cells were maintained in an incubator (37°C, 5% CO_2) in Dulbecco's modified Eagle's medium (containing 110 mg/l pyruvate and 564 mg/l L-glutamine) supplemented with 10% FBS and 0.5% penicillin/streptomycin (nt-HEK cells) or 1% G418-sulfate as a selection media (hTRPA1-HEK and hTRPV1-HEK cells). Transient expression of hTRPA1 was achieved by 24-hour incubation using a BacMam vector (3–5%; kind gift from Dr. M. A. Alexander, GlaxoSmithKline, King of Prussia, PA). Transient expression of hTRPA1 was used for all studies except for the MitoTracker imaging studies that instead used the stably transfected hTRPA1-HEK cell line. Cells were removed from their culture flasks by treatment with Accutase (Innovative Cell Technologies, San Diego, CA), then plated onto poly-D-lysine-coated coverslips, incubated at 37°C, and used within 24 hours.

Fluorescent Ca^{2+} Imaging. Cells were studied for changes in $[Ca^{2+}]_i$ with Fura-2 AM. Neuron-covered coverslips were incubated (37°C) with Fura-2 AM (8 μM, for 30 minutes) in L-15 media containing 10% FBS. HEK293-covered coverslips were incubated (at 37°C) in Dulbecco's modified Eagle's medium (containing 110 mg/l pyruvate and 564 mg/l L-glutamine, supplemented with 10% FBS) with Fura-2 AM (8 μM, for 30 minutes). For imaging, the coverslip was placed in a custom-built heated chamber (bath volume of 300 μl) and superfused by gravity at 8 ml/min with Locke solution [35°C; composition (mM): 136 NaCl, 5.6 KCl, 1.2 $MgCl_2$, 2.2 $CaCl_2$, 1.2 NaH_2PO_4, 14.3 $NaHCO_3$, 10 dextrose (gassed with 95% O_2–5% CO_2, pH 7.3–7.4)] for 10 minutes before and throughout each experiment. Changes in $[Ca^{2+}]_i$ were monitored by sequential dual excitation, 340 and 380 nm (emission 510 nm), measured by digital microscopy

(CoolSnap HQ2; Photometrics, Surrey, BC, Canada), and analyzed by specialized software (Nikon Elements; Nikon, Melville, NY). The ratio images were acquired every 6 seconds. At the end of the dissociated neuronal studies, neurons were exposed to KCl (75 mM, 60 seconds) to confirm voltage sensitivity. At the end of all Fura-2 AM experiments, cells were exposed to ionomycin (5 μM, 60 seconds) to obtain a maximal response. Only one antimycin A treatment was used per preparation. Concentration response curves represent unpaired observations.

For the analysis of $[Ca^{2+}]_i$, we used the excitation ratio 340 nm/380 nm and related all measurements to the peak positive response in each cell. This approach bypasses the conversion of ratiometic responses into absolute $[Ca^{2+}]_i$ using Tsien parameters; thus, we avoided the requirements for calibrating the Fura-2 R_{min}, R_{max}, K_d, and β values for each recorded cell. Given that mammalian cells are heterogeneous with respect to their de-esterification of Fura-2 AM following uptake, raw ratiometric responses should not be compared quantitatively between individual cells. Thus we have chosen to normalize ratiometric responses at each timepoint in each cell to its maximum $[Ca^{2+}]_i$ (evoked by the Ca^{2+} ionophore ionomycin)—data were presented as the percentage change in 340 nm/380 nm ratio (R): response at time (x) = $100 \times (R_x - R_{bl})/(R_{max} - R_{bl})$, where R_x was the 340 nm/380 nm ratio of the cell at a given time point, R_{bl} was the cell's mean baseline 340 nm/380 nm ratio measured over 60 seconds, and R_{max} was the cell's peak 340 nm/380 nm ratio. This normalization allows for quantitative comparisons between cells (Taylor-Clark et al., 2008a,b, 2009). Only cells that had low $[Ca^{2+}]_i$ at baseline ($R < 1.3$) and yielded a robust response to the positive control were included in analyses. Data are presented in the text as mean peak response as a percentage of ionomycin peak or, for the inhibitor/knockout studies, as the mean response against time for the duration of antimycin A treatment (as a percentage of ionomycin peak). For concentration-response data, the pooled unpaired data were fitted with nonlinear regression curve fitting software (Prism; GraphPad Software, La Jolla, CA) using the following equation: y = minimum + (maximum – minimum) / 1 + 10^[(log EC_{50} – x) × Hill slope)], where y is the normalized response and x = log [antimycin A]. EC_{50} values mentioned in the text refer to 50% response of antimycin A's maximum response.

Patch-Clamp Electrophysiology. Recordings from nt-HEK, HEKs transiently expressing hTRPA1, and hTRPV1-HEK cells were made at room temperature (20–23°C) using whole-cell, perforated patch-clamp, or single-channel recording techniques as previously described (Taylor-Clark et al., 2008b, 2009). Membrane currents were recorded and analyzed using a MultiClamp 700B amplifier, Digidata 1440A and pClamp 10 acquisition software (Molecular Devices, Sunnyvale, CA). Current signals were sampled at 100 KHz and filtered at 5 KHz (using an 8-pole Bessel filter) for whole-cell recording or sampled at 2 KHz and filtered at 0.1 KHz for single-channel recording.

Whole-Cell and Perforated Patch Recording. Patch pipettes were fabricated from 1.5-mm o.d., 1.1-mm i.d. borosilicate glass (Sutter Instrument Co., CA) and fire-polished. Pipettes for whole-cell (3–5 MΩ) or perforated-patch recording (1–3 MΩ) were filled with solution composed of (mM): 130 CsCl, 1 $CaCl_2$, 2 $MgCl_2$, 10 HEPES, 10 dextrose, 11 EGTA, and 5 Na-triphosphate; adjusted to pH 7.2 with NaOH. Na-triphosphate was used to prevent rundown of TRPA1 responses (Kim and Cavanaugh, 2007). Perforation was achieved using 5 μg/ml gramicidin. Cells on a coverslip were superfused at 8 ml/min with HEPES-buffered bath solution [composition (mM): 154 NaCl, 4.7 CsCl, 1.2 $MgCl_2$, 0.01 $CaCl_2$, 10 HEPES, 5.6 dextrose; adjusted to pH 7.4 with NaOH]. Cells were voltage-clamped at 0 mV and 500-millisecond voltage ramps from –80 mV to +80 mV were applied every second. Currents evoked by voltage ramps were analyzed at –70 mV or +70 mV. Only one antimycin A treatment was used per cell. TRP channel inhibitors were added 2 minutes after antimycin A to indicate TRP-dependent currents (paired experiments).

Single-Channel Inside-Out Patch Recording. Patch pipettes were fabricated from 1.5-mm o.d., 0.75-mm i.d. borosilicate glass, the tips coated in Sylgard 184 (Dow Corning, Midland, MI) and fire-polished. Pipettes, when filled, had resistances of 5–9 MΩ. The bath and pipette solution comprised (in mM): 126 NaCl, 4 KCl, 2 EGTA (no Ca^{2+} added), 1 $MgCl_2$, 10 HEPES, 5 glucose, and 5 Na-triphosphate [to prevent TRPA1 rundown (Kim and Cavanaugh, 2007)]; adjusted to pH 7.3 with NaOH. The patch was held at 0 mV, then the presence of TRP channels was confirmed by conductances observed in a series of voltage steps: 100 milliseconds from –60 mV to +60 mV in 20-mV steps. Excised patches were held at +40 mV and current recordings made for 10 minutes. Antimycin A was applied for 3 minutes followed by AITC or capsaicin for 1–3 minutes. Digitized data were analyzed (pClamp 10.0; Molecular Devices) to obtain channel activity (NP_o, in which N is the number of channels in the patch and P_o is the open probability) and amplitude histograms for single-channel conductance. Due to the variability in the frequency of single-channel openings under control conditions, the final data are expressed as the relative change in open probability upon drug treatment. Only one antimycin treatment was used per patch. ROS scavengers were added prior to antimycin A treatment (unpaired comparison with control).

Imaging of Membrane-Bound Mitochondria. nt-HEK293, hTRPA1-HEK, and hTRPV1-HEK on coverslips were incubated for 30 minutes at 37°C with MitoTracker Orange CMTMRos (250–500 ng/ml; Life Technologies, Carlsbad, CA). Cells were then perfused using whole-cell bath solution and inside-out excised patches pulled using pipettes backfilled with whole-cell pipette solution as described above. Fluorescence was observed using an X-Cite 120Q fluorescent light source (EXFO Inc., Quebec City, QC, Canada) and a rhodamine filter. Images were obtained using a Retiga Exi Fast 1394 camera and captured using QCapture software (QImaging, Surrey, BC, Canada).

Statistical Analysis. Data were analyzed using GraphPad software. Where appropriate paired or unpaired Student's t-tests were used. A P value less than 0.05 was taken as significant. All data were expressed as mean ± S.E.M. unless otherwise noted.

Chemicals. AITC, antimycin A, catalase, cinnamaldehyde, glutathione, MnTMPyP, and superoxide dismutase were purchased from Sigma-Aldrich (St. Louis, MO). Tempol, HC-030031, ruthenium red, and capsaicin were purchased from Tocris (Ellisville, MO). Fura-2 AM was purchased from TEFLabs (Austin, TX). 5′-Iodoresiniferatoxin was purchased from Alomone Laboratories (Jerusalem, Israel).

Results

Mitochondrial Modulation Activates Nociceptive Airway Vagal Nerves. To test whether modulation of nerve terminal mitochondria play a role in vagal sensory nerve activation we used the selective ETC complex III inhibitor antimycin A. Antimycin A inhibits the Q_i site on complex III, redirecting electrons along the transport chain, and causing the incomplete reduction of available O_2, thus resulting in superoxide formation in isolated mitochondria (10 nM to 10 μM) (Potter and Reif, 1952; Slater, 1973; Turrens et al., 1985; Gyulkhandanyan and Pennefather, 2004; Stowe and Camara, 2009) and intact cells (0.5–50 μM) (Li et al., 2003; Kim and Usachev, 2009; Liu et al., 2010; Gonzalez-Dosal et al., 2012). To study the mitochondria that are densely packed within bronchopulmonary sensory nerve terminals (von During and Andres, 1988), we have used a mouse ex vivo lung-vagal ganglia preparation in which drug treatments are perfused through the isolated lung and the action potential discharge of individual bronchopulmonary sensory nerves is recorded by an extracellular electrode micro-positioned in the vagal ganglia. The majority of bronchopulmonary sensory fibers are slowly conducting nociceptive c-fibers that serve to protect the airways from noxious stimuli by evoking defensive reflexes

(Carr and Undem, 2003). We have previously shown that these nociceptive fibers express TRPV1 and TRPA1 channels (Nassenstein et al., 2008; Taylor-Clark et al., 2008a, 2009). Here, bronchopulmonary fibers were characterized by conduction velocity and responses to selective agonists for TRPA1 (cinnamaldehyde, 300 μM; and AITC, 300 μM), and TRPV1 (capsaicin, 1 μM) using concentrations previously shown to be selective for specific TRP channels (Caterina et al., 1997; Kollarik et al., 2003; Jordt et al., 2004; Macpherson et al., 2007; Nassenstein et al., 2008). As expected, capsaicin activated the vast majority of slowly conducting c-fibers (conduction velocity $<$0.7 m/s, mean peak response 14.2 $\pm$ 1.9Hz) (Kollarik et al., 2003). Approximately half of these nociceptive-like fibers (46/86) also responded to TRPA1 agonists. Fast conducting ($>$0.7 m/s) fibers did not respond to either TRPA1 or TRPV1 agonists, which is consistent with previous reports describing the non-nociceptive nature of fast conducting airway nerves (Kollarik et al., 2003; Undem et al., 2004).

We chose the concentration of 20 μM antimycin A for these neuronal studies based upon previous studies in intact cells (Li et al., 2003; Kim and Usachev, 2009; Liu et al., 2010; Gonzalez-Dosal et al., 2012). This concentration is expected to produce near maximal inhibition of complex III and evoke substantial superoxide production. Antimycin A (20 μM) caused robust action potential discharge in slowly-conducting nociceptive (i.e., TRPV1-expressing) sensory nerves (Fig. 1A). The peak discharge in response to antimycin A in TRPA1-expressing nociceptors (7.5 $\pm$ 1.9 Hz, n = 17) was significantly higher than in nociceptors not expressing TRPA1 (2.5 $\pm$ 1.0 Hz, n = 22, $P < 0.02$). Antimycin A failed to activate non-nociceptors (0.5 $\pm$ 0.4 Hz, n = 11). These results suggest that acute modulation of sensory nerve terminal mitochondria selectively activates a major subset of nociceptive nerves innervating the airways. Regardless of conduction velocity or sensitivity to TRP channel ligands, these bronchopulmonary fibers continued to demonstrate electrical excitability up to 1 hour after antimycin A treatment.

Next we tested whether antimycin A-induced nerve activation is due to direct effects on the nerve mitochondria or is mediated through its actions on neighboring cells in the lung. We studied the effect of mitochondrial modulation on dissociated vagal sensory neurons using Ca^{2+} imaging. Preliminary studies demonstrated that 80% of dissociated vagal neurons were activated by AITC (100 μM) and 74% by capsaicin (1 μM) (unpublished data), similarly to our previous studies (Taylor-Clark et al., 2008a,b, 2009). Antimycin A (20 μM) increased $[Ca^{2+}]_i$ in 298 out of 320 neurons (peak response 36.0 $\pm$ 1.5% of ionomycin response), comparable to the magnitude of AITC and capsaicin responses, indicating that antimycin A directly activated sensory neurons in an environment devoid of other cell types (e.g., epithelial cells, smooth muscle cells) (Fig. 1B). In the absence of extracellular Ca^{2+}, antimycin A failed to increase $[Ca^{2+}]_i$ in dissociated vagal sensory neurons (n = 59), indicating that antimycin A increases $[Ca^{2+}]_i$ through the gating of Ca^{2+}-permeable ion channels in the plasma membrane (unpublished data).

TRPA1 and TRPV1 Channels Are Critical for Mitochondrial Modulation-Induced Nerve Activation. Given that acute mitochondrial modulation by antimycin A is likely to produce ROS and that ROS are capable of activating TRPA1 (Andersson et al., 2008; Sawada et al., 2008; Takahashi et al., 2008) and TRPV1 (Susankova et al., 2006; Taylor-Clark et al., 2008a; Chuang and Lin, 2009), we hypothesized that the selective activation of vagal nociceptors by antimycin A was due to the indirect gating of these channels. We first addressed this hypothesis using the selective TRPA1 inhibitor HC-030031 [IC_{50} ~1 μM, (McNamara et al., 2007)] and the selective

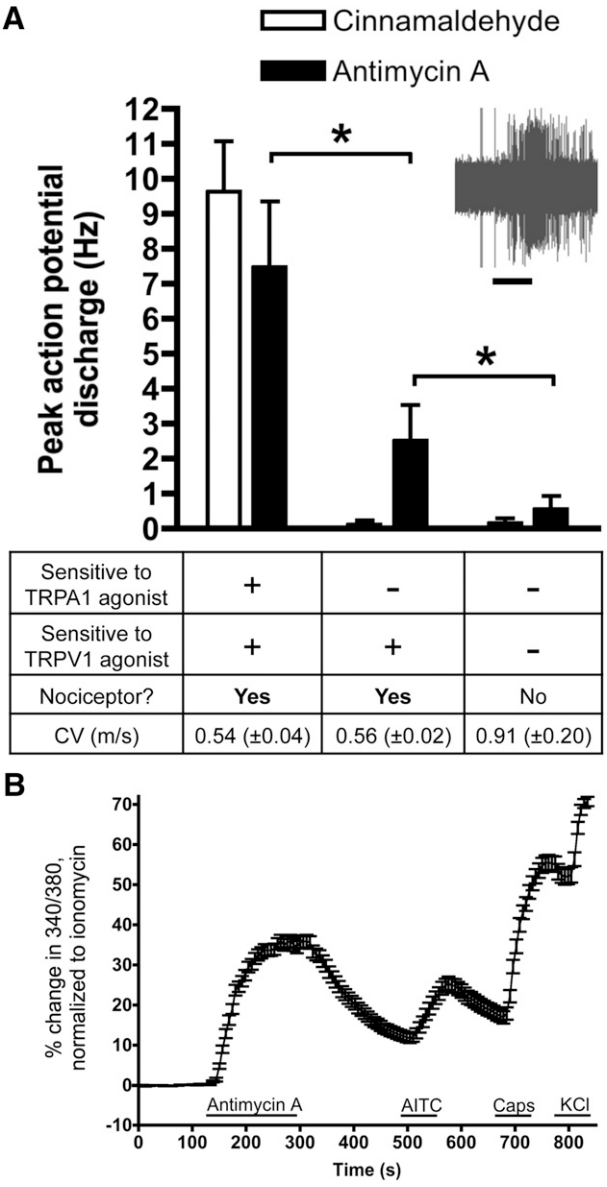

Sensitive to TRPA1 agonist	+	-	-
Sensitive to TRPV1 agonist	+	+	-
Nociceptor?	**Yes**	**Yes**	No
CV (m/s)	0.54 (±0.04)	0.56 (±0.02)	0.91 (±0.20)

Fig. 1. Antimycin A activates nociceptive vagal sensory neurons. (A) Mean $\pm$ S.E.M. peak action potential discharge from individual wild-type bronchopulmonary C-fibers in response to cinnamaldehyde (300 μM) and antimycin A (20 μM). Bronchopulmonary C-fibers were grouped according to their response to TRPA1 [cinnamaldehyde and/or AITC (300 μM)] and TRPV1 agonists (capsaicin, 1 μM). Mean $\pm$ S.E.M. conduction velocity (CV) is also shown. Sensitivity to TRP agonists and a conduction velocity $<$0.7 m/s was used as an indicator that the studied nerve is nociceptive (Kollarik et al., 2003; Nassenstein et al., 2008). *Significant difference in antimycin A response between groups ($P < 0.05$). Inset, representative trace showing action potential discharge to antimycin A (blocked line denotes 10-second application) in an individual TRPA1-expressing bronchopulmonary C-fiber. (B) Mean $\pm$ S.E.M. Ca^{2+} responses of dissociated wild-type vagal ganglia neurons (n = 298) in response to antimycin A (20 μM), AITC (100 μM), capsaicin (Caps, 1 μM), and KCl (75 mM). Blocked lines depict the duration of drug application.

TRPV1 inhibitor 5′-iodoresiniferatoxin [I-RTX; IC_{50} ~5 nM (Wahl et al., 2001)]: we have previously shown these inhibitors selectively and potently inhibit AITC (TRPA1)- and capsaicin (TRPV1)-induced responses in sensory nerves, respectively (Taylor-Clark et al., 2008a,b). Three-minute perfusion pretreatment with the selective TRPA1 inhibitor HC-030031 (30 μM) significantly decreased antimycin A-induced Ca^{2+} influx (mean response 13.3 ± 1.0%, $n = 171$, $P < 0.05$) compared with control (mean response 26.3 ± 1.1%, $n = 298$) in dissociated vagal neurons (Fig. 2, A and C). As expected HC-030031 abolished AITC-induced neuronal activation but had no effect of capsaicin responses (data not shown). Three-minute perfusion pretreatment with the selective TRPV1 inhibitor I-RTX (500 nM) also reduced antimycin A-induced neuron activation, albeit to a lesser extent (mean response 17.3 ± 2.2%, $n = 165$ $P < 0.05$). As expected I-RTX abolished capsaicin-induced neuronal activation but had no effect of AITC responses (unpublished data). These findings were supported by complementary knockout studies (Fig. 2, B and C). Antimycin A evoked significantly less Ca^{2+} influx in vagal sensory neurons derived from $TRPA1^{-/-}$ mice (mean response 11.3 ± 1.7%, $n = 81$, $P < 0.05$) compared with wild-type neurons. Responses to antimycin A were also reduced in vagal sensory neurons from $TRPV1^{-/-}$ mice (mean response 21.3 ± 1.4%, $n = 137$, $P < 0.05$). There was no significant difference between the pharmacological inhibition and genetic ablation of TRPA1 in decreasing antimycin A-induced Ca^{2+} influx. There was also no significant difference between the pharmacological inhibition and genetic ablation of TRPV1 in decreasing antimycin A-induced Ca^{2+} influx. These studies suggest that both TRPA1 and TRPV1 contribute to antimycin A-induced neuronal responses. Furthermore, antimycin A-induced activation was completely abolished in $TRPA1^{-/-}$ mouse vagal neurons in the presence of TRPV1 inhibitor I-RTX (mean 0.0 ± 0.8%, $n = 50$, $P < 0.05$) (Fig. 2, B and C). Thus the Ca^{2+} influx evoked by acute mitochondrial modulation is dependent mostly on the activation of TRPA1 and, to a lesser extent, TRPV1.

We next studied the mechanism underlying the action potential discharge from bronchopulmonary C-fiber terminals evoked by antimycin A (Fig. 3). Again, fibers were identified as "TRPA1-expressing" by their response to selective TRPA1 ligands (cinnamaldehyde and AITC) and as "nociceptors" by their conduction velocity (and by capsaicin sensitivity for wild-type C-fibers). We hypothesized that TRPA1 would contribute to the antimycin A-induced activation of TRPA1-expressing bronchopulmonary C-fibers. Indeed, 10-minute pretreatment of TRPA1-expressing nociceptors from wild-type mice with TRPA1 channel antagonist HC-030031 (30 μM) decreased antimycin A-induced action potential discharge (peak discharge of 1.6 ± 0.7 Hz, $n = 9$, $P < 0.01$) compared with control (7.5 ± 1.9 Hz), suggesting that TRPA1 channels are critical to the initiation of action potentials from the nerve terminal (Fig. 3, left). Consistent with our hypothesis indicating that neuronal mitochondrially-derived ROS (see below) are sufficient to mediate antimycin A-induced nerve activation, 10-minute pretreatment with a membrane-impermeable antioxidant glutathione (GSH, 3 mM) had no effect on antimycin A-induced action potential discharge (7.8 ± 2.6 Hz, $n = 5$, $P > 0.4$). Our studies also demonstrated a possible role of TRPV1 in the nerve terminal responses to mitochondrial modulation. Antimycin A evoked decreased action potential discharge from TRPA1-expressing fibers from $TRPV1^{-/-}$ mice (peak discharge 4.3 ± 1.2 Hz, $n = 10$, $P = 0.08$), although this did not reach significance compared with controls (Fig. 3, middle). However, in wild-type nociceptors that did not express TRPA1 (as determined by a lack of response to TRPA1 selective agonist), the TRPV1 inhibitor I-RTX (1 μM) produced a significant reduction in antimycin A-induced nerve activation (peak discharge 0.6 ± 0.3 Hz, $n = 10$, $P < 0.05$; compared with 2.5 ± 1.0 Hz, $n = 22$ without I-RTX), indicating the residual non-TRPA1-mediated antimycin A-induced action potential discharge was due to the activation of TRPV1 (Fig. 3, right). Therefore, similar to findings in dissociated vagal neurons, the action potential discharge in bronchopulmonary C-fibers evoked by antimycin A was due to the activation of TRPA1 and, to a lesser extent, TRPV1.

Mitochondrial Modulation Activates TRPA1 and TRPV1 in HEK293 Cells. TRP channels are membrane-bound polymodal cation-permeable channels that can be activated by multiple stimuli (Patapoutian et al., 2009). We further studied the interaction of mitochondrial function and TRPA1 and TRPV1 in HEK293 cells. At concentrations

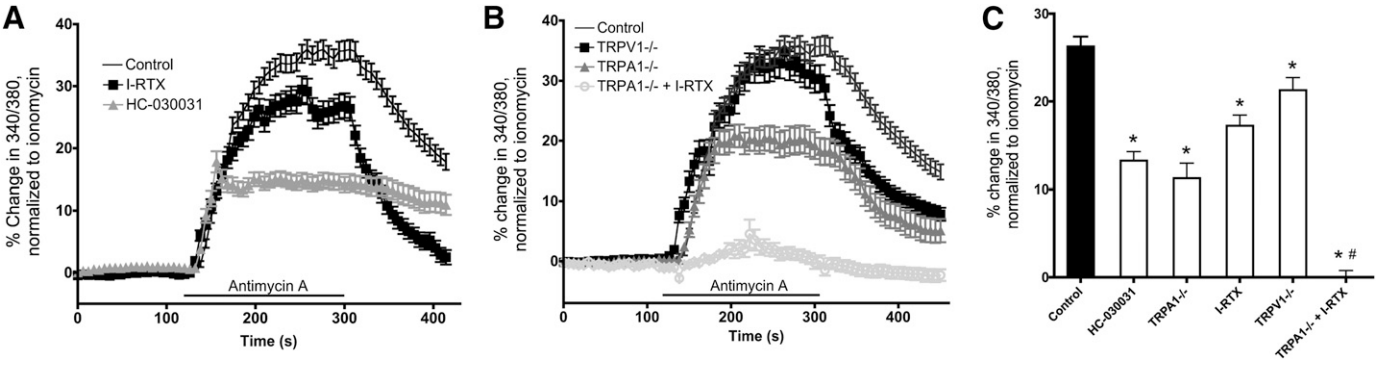

Fig. 2. Contribution of TRPA1 and TRPV1 to antimycin A-induced Ca^{2+} influx in vagal neurons. (A) Mean ± S.E.M. Ca^{2+} responses of dissociated wild-type vagal sensory neurons in response to antimycin A (20 μM). Control conditions (black line, $n = 298$), in the presence of 1 μM I-RTX (black squares, $n = 165$) and 30 μM HC-030031 (gray triangles, $n = 171$). (B) Mean ± S.E.M. Ca^{2+} responses in control wild-type neurons (black line, $n = 298$), $TRPV1^{-/-}$ neurons (black squares, $n = 137$), $TRPA1^{-/-}$ neurons (gray triangles, $n = 81$), and $TRPA1^{-/-}$ neurons in the presence of 1 μM I-RTX (gray rings, $n = 50$). Blocked lines depict the duration of antimycin A treatment. (C) Mean ± S.E.M. Ca^{2+} response of mouse vagal dissociated neurons during antimycin A treatment (228 seconds). *Significant reduction compared with control ($P < 0.05$); #significant reduction compared with $TRPA1^{-/-}$ neurons ($P < 0.05$).

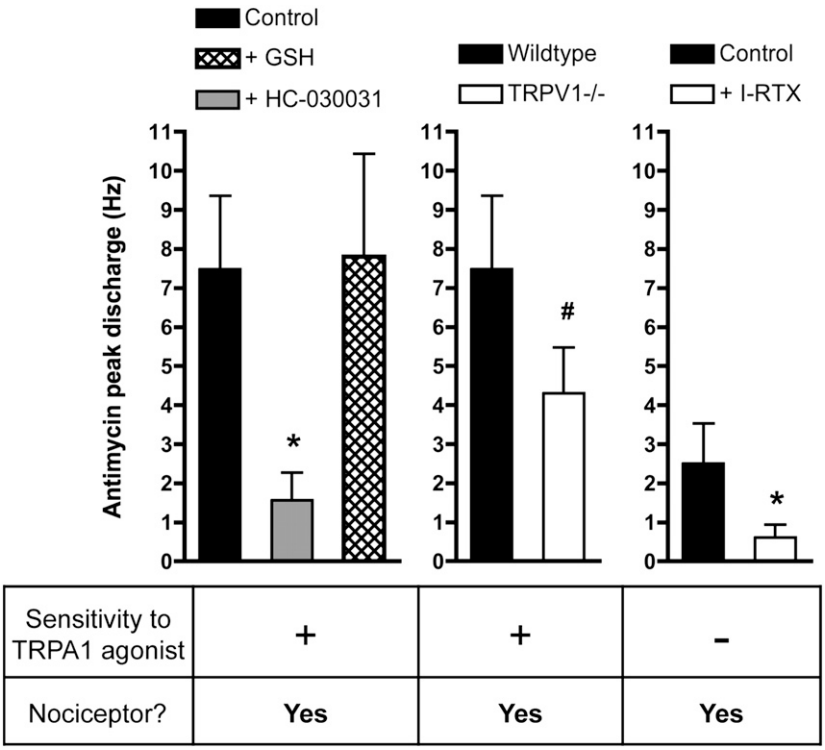

Fig. 3. Contribution of TRPA1 and TRPV1 to the activation of bronchopulmonary C-fibers by antimycin A. Mean ± S.E.M. peak action potential discharge from individual bronchopulmonary C-fibers in response to antimycin A (20 μM). Bronchopulmonary C-fibers were grouped according to their response to TRPA1 agonists [cinnamaldehyde (300 μM) and/or AITC (300 μM); data not shown]. Data in all columns only includes *nociceptive* wild-type and TRPV1$^{-/-}$ C-fibers, defined by conduction velocity and (only for wild-type C-fibers) sensitivity to capsaicin (1 μM; unpublished data). Left, responses in control wild-type TRPA1-expressing fibers (black column) are compared with responses in the presence of 30 μM HC-030031 (gray column) and 1 mM GSH (hatched column). Middle, responses in control wild-type TRPA1-expressing fibers (black column) are compared with responses in TRPA1-expressing TRPV1$^{-/-}$ C-fibers (white column). Right, responses in control wild-type fibers not expressing TRPA1 (black column) are compared with responses in the presence of 1 μM I-RTX. *Significant reduction compared with control ($P < 0.05$).

sufficient to selectively inhibit ETC complex III in intact cells (0.5–20 μM) (Li et al., 2003; Kim and Usachev, 2009; Liu et al., 2010; Gonzalez-Dosal et al., 2012), antimycin A caused an increase in 340 nm/380 nm ratio in Fura 2 AM-loaded HEK293 cells transiently expressing hTRPA1, indicating an increase in $[Ca^{2+}]_i$ and TRPA1 activation (Fig. 4, A and B). The effect of antimycin A on TRPA1 channel activation was concentration-dependent and the relationship was fitted with nonlinear regression, indicating an apparent EC_{50} of 1.8 μM (95% confidence interval, 1.4–2.4 μM), a Hill slope of 2.8 (95% confidence interval 0.5–5.2), and an R^2 goodness-of-fit of 0.99. Antimycin failed to activate nt-HEK cells. Consistent with the activation of the cation-permeable TRP channel, the antimycin A-induced increase in $[Ca^{2+}]_i$ in HEKs expressing hTRPA1 was dependent on Ca^{2+} influx—the response was absent in the absence of external calcium ($n = 59$, unpublished data). Studies of stably transfected hTRPV1-HEK cells indicated that TRPV1 was also activated by antimycin A in a concentration-dependent manner, albeit to a lesser extent (Fig. 4, A and B).

We investigated the effect of antimycin A on TRP channel currents using whole-cell patch clamp electrophysiology. To maximize the putative TRP currents following antimycin A treatment we chose to use 10 μM antimycin A (identified as a maximal dose in our Ca^{2+} imaging studies of HEK293 cells). To prevent rundown of TRPA1 currents, we added 5 mM Na-triphosphate to the pipette solution (Kim and Cavanaugh, 2007). In these studies, outwardly rectifying currents (reversing at 0 mV) were evoked by AITC and capsaicin as expected: HEK cells transfected with hTRPA1 responded to AITC [30 μM, control: –89 ± 20 pA at –70 mV, 127 ± 19 pA at +70 mV; AITC: –1027 ± 184 at –70 mV, 1906 ± 251 pA at +70 mV ($P < 0.01$)] and hTRPV1-HEK cells responded to capsaicin [300 nM, control: –41 ± 5 pA at –70 mV, 93 ± 11 pA at +70 mV; capsaicin: –389 ± 128 at –70 mV, 948 ± 194 pA at +70 mV ($P < 0.01$)]. Antimycin A (10 μM) failed to increase currents in nt-HEK cells ($n = 5$) (Fig. 5A). However, we found that antimycin A evoked outwardly rectifying currents in HEKs transfected with TRPA1 ($n = 16$, $P < 0.001$) that were subsequently inhibited by the selective TRPA1 inhibitor HC-030031 (30 μM, $n = 6$, $P < 0.01$) (Fig. 5B). In whole-cell patch clamp recordings of hTRPV1-HEK cells, antimycin A (10 μM) failed to evoke detectable currents ($n = 5$, unpublished data). However in gramicidin-perforated patch clamp recordings antimycin A (10 μM) evoked small but significant outwardly rectifying currents ($n = 7$, $P < 0.05$) that were subsequently inhibited by the TRP channel blocker ruthenium red (30 μM, $P < 0.05$) (Fig. 5C). In addition, in one cell, antimycin A-induced hTRPV1 currents were abolished by the selective TRPV1 inhibitor I-RTX (500 nM, unpublished data). The lack of detectable currents in whole-cell patch clamp recordings of hTRPV1-HEK cells may be due to the combination of a weak activation of TRPV1 following acute mitochondrial modulation and the dilution of soluble factors required for the channel activation.

Mechanism of Antimycin A-Induced TRPA1 Activation. Given the preferential role of TRPA1 in mitochondrial modulation-induced nociceptive neuronal activation, we further investigated the mechanism underlying the TRPA1 activation. TRPA1 can be activated through multiple mechanisms, including N-terminal cysteine modification (by ROS and lipid peroxidation products) (Hinman et al., 2006; Macpherson et al., 2007), intracellular Ca^{2+} (Zurborg et al., 2007), and noxious cold temperatures (Story et al., 2003). Selective inhibition of the Q_i site in mitochondrial ETC complex III by antimycin A (≤50 μM) causes mitochondrial membrane potential depolarization and substantial superoxide production (Potter and Reif, 1952; Slater, 1973; Turrens et al., 1985; Gyulkhandanyan and Pennefather, 2004; Stowe and Camara, 2009). Given TRPA1's sensitivity to ROS and

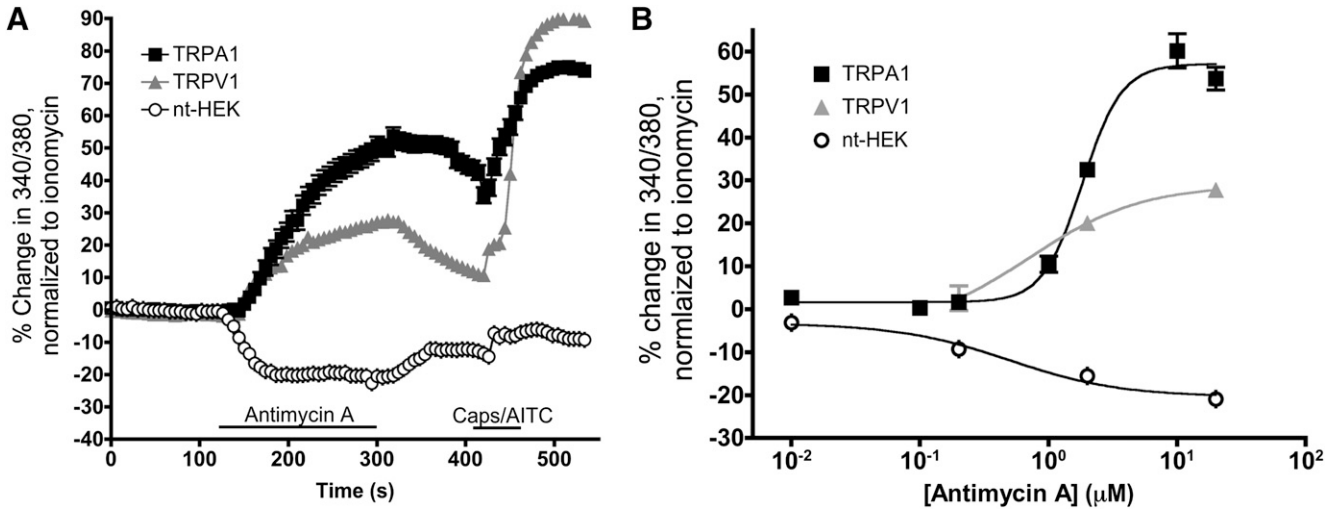

Fig. 4. Antimycin A increases $[Ca^{2+}]_i$ in hTRPA1- and hTRPV1-expressing cells. (A) Mean ± S.E.M. Ca^{2+} responses against time in HEKs transiently expressing hTRPA1 (black squares, n = 269), hTRPV1-HEK cells (gray triangles, n = 470), and nt-HEK cells (black rings, n = 334) in response to antimycin A (20 μM) and either AITC (TRPA1 and nt-HEK, 100 μM) or capsaicin (Caps, 1 μM). Blocked lines depict the duration of drug treatment. (B) Concentration-response relationships for antimycin A in HEKs transiently expressing hTRPA1 [black squares, n numbers (reading from lowest to highest concentration): 12, 22, 223, 125, 793, 118, 269); hTRPV1-HEK cells [gray triangles, n numbers (reading from lowest to highest concentration): 146, 912, 470]; and nt-HEK cells [black rings, n numbers (reading from lowest to highest concentration): 30, 120, 238, 334]. S.E.M may be hidden within the symbols. Data were fitted by nonlinear regression. EC_{50} for antimycin A-induced TRPA1 activation was determined to be 1.8 μM.

downstream lipid peroxidation products we therefore hypothesized that antimycin A activated TRPA1 indirectly via the mitochondrial production of ROS. TRPA1 is rapidly activated following antimycin A treatment (see Fig. 4). Given the difficulty in complete elimination of evoked mitochondrial ROS within this limited timeframe (and prior to TRPA1 activation), we chose to use 2 μM antimycin A (approximately EC_{50} for TRPA1 activation) in the following mechanistic studies.

We first addressed this hypothesis using myxothiazol, an inhibitor of the Q_o site on complex III. Inhibition of Q_o causes mitochondrial membrane potential depolarization but only very mild superoxide production (Turrens et al., 1985; Gyulkhandanyan and Pennefather, 2004; Tretter et al., 2007). Furthermore, selective inhibition of Q_o (myxothiazol) substantially reduces subsequent superoxide production evoked by inhibition of the Q_i site (antimycin A) (Turrens et al., 1985; Gyulkhandanyan and Pennefather, 2004; Tretter et al., 2007). Myxothiazol (200 nM) evoked a mild initial increase in $[Ca^{2+}]_i$ in both nt-HEK (n = 68) and HEK293 cells transiently expressing hTRPA1 (n = 137), although this response decreased to a greater extent in nt-HEK upon washout. It is possible that the TRPA1-mediated responses immediately following myxothiazol washout are due to limited ROS production by the Q_o site inhibitor. Following myxothiazol treatment, 2 μM antimycin A-induced TRPA1 activation was reduced (peak response 10.8 ± 2.0% ionomycin) compared with controls (peak response 35.6 ± 2.1% ionomycin, n = 103, $P < 0.05$) (Fig. 6A). Importantly, direct activation of hTRPA1 by AITC (100 μM) was unaffected by myxothiazol pretreatment. Thus we conclude that antimycin A indirectly activates TRPA1 in a manner that is dependent on superoxide production from the Q_i site of complex III.

Superoxide can be converted into H_2O_2 by superoxide dismutase (SOD) enzymes in both the mitochondrial matrix (SOD2) and the cytosol (SOD1); H_2O_2 is then broken down by catalase. Both superoxide and H_2O_2 have been shown to activate TRPA1 (Andersson et al., 2008; Sawada et al., 2008; Takahashi et al., 2008). To investigate the role of ROS in mitochondrial modulation-induced TRPA1 activation we used tempol [SOD mimetic (Krishna et al., 1996)] and MnTMPyP [combined SOD and catalase mimetic (Faulkner et al., 1994; Day et al., 1997)] (Fig. 6, B and C). For tempol pretreatment, cells were first incubated for 90 minutes in 1 mM tempol, followed by 10-minute perfusion pretreatment with 100 μM tempol. Tempol had little effect on 2 μM antimycin A-induced TRPA1 activation (n = 213). Fifteen-minute perfusion pretreatment with MnTMPyP (50 μM) reduced antimycin A-induced TRPA1 activation: mean response over 180 seconds was 16.8 ± 2.9% (n = 58) compared with 26.9 ± 0.9% in controls (n = 628, $P < 0.05$). A combination of tempol and MnTMPyP further reduced antimycin A-induced TRPA1 activation (mean response over 180 seconds was 6.7 ± 1.6%, n = 55, $P < 0.05$), indicating that ROS were critical for the activation of TRPA1 following mitochondrial modulation. None of the tempol/MnTMPyP treatments reduced direct activation of hTRPA1 by AITC (100 μM).

ROS can activate TRPA1 directly through reversible modification of N-terminal cysteines (Andersson et al., 2008; Takahashi et al., 2008). In addition, ROS are able to initiate peroxidation of unsaturated phospholipids (Karihtala and Soini, 2007), increasing the local concentration of compounds with α,β-unsaturated carbonyl moieties (e.g., 4-hydoxynonenal) that directly activate TRPA1 through modification of N-terminal cysteines via Michael addition reactions (Trevisani et al., 2007). We investigated the mechanism by which ROS evoked by mitochondrial modulation activated TRPA1 (direct versus indirect) using the reducing agent dithiothreitol (DTT). DTT prevents and reverses sulfhydryl group oxidation/disulfide bond formation of exposed cysteine residues by hydrogen peroxide and other ROS (Getz et al., 1999), and has previously been shown to prevent and reverse TRPA1 activation by these compounds (Andersson et al., 2008; Sawada et al., 2008; Takahashi et al., 2008). However, DTT has no effect on cysteine modifications by α,β-unsaturated

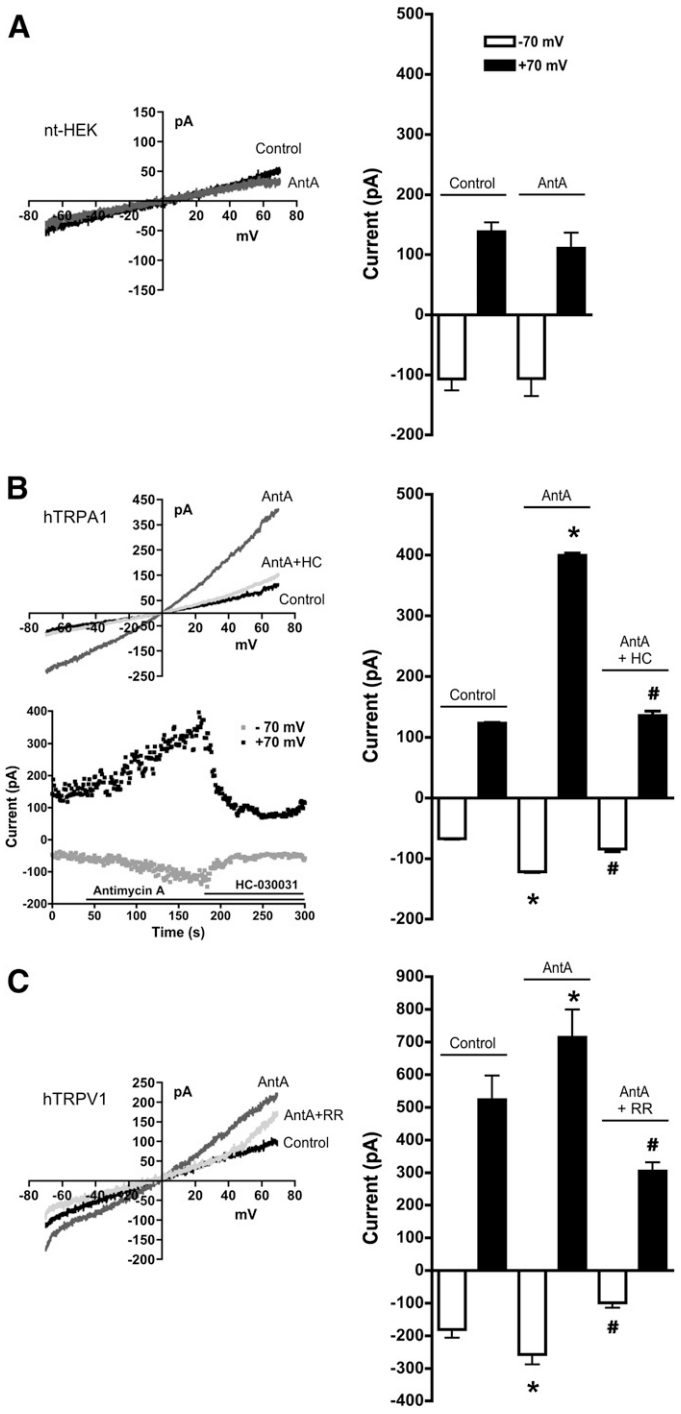

Fig. 5. Antimycin A induces the activation of TRPA1 and TRPV1 channels. Whole-cell currents evoked under control conditions (black line) and during antimycin A (AntA; 10 μM, dark gray line) treatment. (A) nt-HEK cells: (left) representative I-V relationship and (right) mean ± S.E.M. currents at –70 (white bars) and +70 mV (black bars). (B) hTRPA1-expressing HEKs without and with HC-030031 (HC, 30 μM, light gray line): representative I-V relationship (upper left), representative current response [(lower left) –70 (gray squares) and +70 mV (black squares)] against time, and mean ± S.E.M. currents at –70 and +70 mV (right). (C) Perforated patch of hTRPV1-expressing HEKs without and with ruthenium red (RR, 30 μM, light gray line): representative I-V relationship (left) and mean ± S.E.M. currents at –70 and +70 mV (right). *Significant increase in currents compared with control conditions ($P < 0.05$); #significant reduction by inhibitor ($P < 0.05$).

carbonyl moieties (Michael reactions) and consequently DTT has no effect on TRPA1 activation by lipid peroxidation products (Macpherson et al., 2007; Andersson et al., 2008; Takahashi et al., 2008). Three-minute perfusion pretreatment with DTT (1 mM) abolished 20-μM antimycin A-induced TRPA1 activation (peak response 2.7 ± 2.4% ionomycin, n = 266) [$P < 0.05$ compared with control: peak response 53.7 ± 2.7% (n = 269)] (Fig. 6D). As expected, neither 1 mM or 10 mM DTT had any effect on AITC-induced TRPA1 activation (Fig. 6E and unpublished data). This data indicates that TRPA1 activation downstream of mitochondrial modulation is not dependent on Michael addition by α,β-unsaturated carbonyl moieties, suggesting a direct (DTT-sensitive) activation by mitochondrially-produced ROS.

Together the myxothiazol, tempol/MnTMPyP, and DTT studies are consistent with ROS mediating mitochondrial modulation-induced TRPA1 activation as opposed to a direct effect of antimycin A on TRPA1 N-terminal cysteines. Direct modification of model thiol groups can be determined using spectrophotometry and Ellman's reagent [5,5′-dithiobis-(2-nitrobenzoic acid) (DTNB)]. Reduction of DTNB using DTT produces 2-nitro-5-thiobenzoate (NTB), which absorbs strongly at 412 nm. NTB is a free thiol group that, when modified by a cysteine-reactive compound, loses its absorption at 412 nm. To confirm that antimycin A does not directly modify thiol groups we compared antimycin A with cinnamaldehyde and iodoacetamide [both direct TRPA1 agonists via cysteine modification (Macpherson et al., 2007)]. Cinnamaldehyde and iodoacetamide eliminated NTB absorption with a second-order rate constant of 1.74 ± 0.1 $M^{-1}s^{-1}$ (n = 7) and 0.25 ± 0.03 $M^{-1}s^{-1}$ (n = 5), respectively [values consistent with previous studies (Chen and Armstrong, 1995)]. Antimycin A had no effect on NTB (second-order rate constant $<0.001\ M^{-1}s^{-1}$, n = 3), indicating antimycin A is not capable of directly modifying thiol groups.

We lastly studied the effect of antimycin A on single TRP channel currents in excised inside-out patches from TRP-expressing HEK cells. To prevent rundown of TRPA1 currents, we added 5 mM Na-triphosphate to the extracellular solution (Kim and Cavanaugh, 2007). We identified stochastic conductances in hTRPA1-expressing cells of 153 picosiemens (pS; S.D. 24 pS, n = 13) at +40 mV, whose open probabilities were increased by AITC (10 μM, n = 5) (Fig. 7, A and B). Similarly, we identified stochastic conductances in hTRPV1-expressing cells of 121 pS (S.D. 66 pS, n = 4) at +40 mV, whose open probabilities were increased by capsaicin (300 nM, n = 4) (Fig. 7, A and B). We predicted that antimycin A would have little effect on excised patches containing TRP channels based on the expectation that excised patches would be devoid of cytosolic organelles. Surprisingly, antimycin A (10 μM) evoked a significant increase in the probability of stochastic conductances in TRPA1 expressing patches (n = 7) consistent with hTRPA1 activation (Fig. 7, C–E). Antimycin A (10 μM) had no effect on excised patches from nt-HEK cells (n = 4) or on the probability of TRPV1 opening in patches from hTRPV1-expressing cells (n = 4). Based on our Ca^{2+} imaging studies, we hypothesized that antimycin A increased TRPA1 single-channel gating downstream of mitochondrial ROS. As such we hypothesized that functional mitochondria, lying close to the HEK293 cell membrane, were taken up along with the excised membrane during the act of inside-out patch excision, as has been previously shown in pancreatic B-cells (Rustenbeck et al., 1999). Using the mitochondrial-specific fluorescent probe

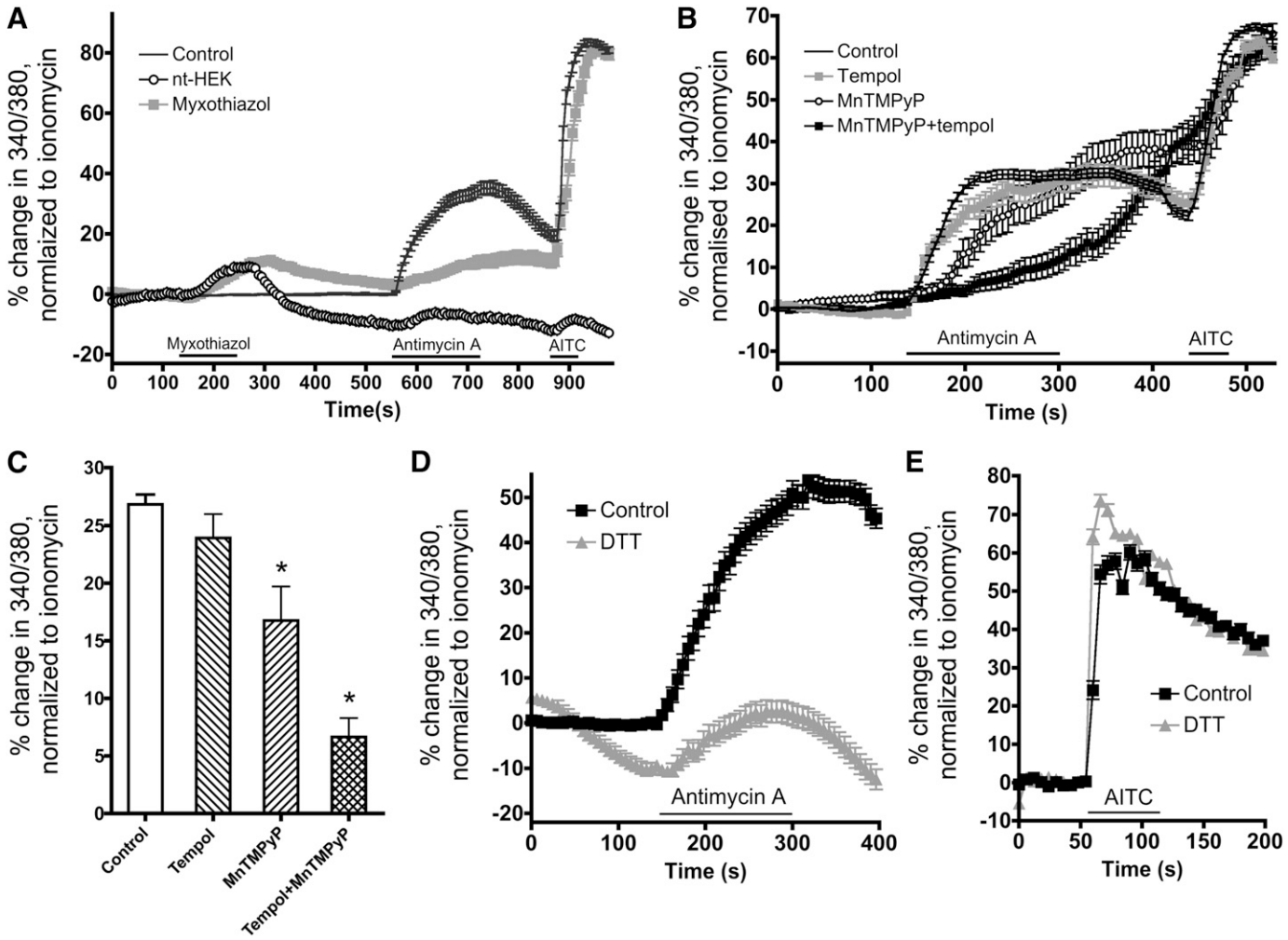

Fig. 6. Antimycin A activates TRPA1 indirectly via the actions of mitochondrially-derived ROS. (A, B) Mean ± S.E.M. Ca^{2+} responses against time in response to antimycin A (2 μM) and AITC (100 μM). (A) Data include HEKs transiently expressing hTRPA1 without (black line, n = 103) and with pretreatment with myxothiazol (200 nM) (gray squares, n = 137), and nt-HEK cells with pretreatment with myxothiazol (black rings, n = 68). (B) Data include HEKs transiently expressing hTRPA1 under control conditions (black line, n = 628), and with pretreatment of tempol (gray squares, 1 mM, n = 213), MnTMPyP (black rings, 50 μM, n = 58), or a combination of tempol and MnTMPyP (black squares, n = 55). (C) Mean ± S.E.M. Ca^{2+} response of HEKs transiently expressing hTRPA1 to antimycin A during tempol/MnTMPyP treatments (180 seconds). *Significant reduction compared with control ($P < 0.05$). (D) Mean ± S.E.M. Ca^{2+} responses of HEKs transiently expressing hTRPA1 in response to antimycin A (20 μM) in control conditions (black squares, n = 269) and in the presence of DTT (1 mM, gray triangles, n = 266). (E) Mean ± S.E.M. Ca^{2+} responses of HEKs transiently expressing hTRPA1 in response to AITC (100 μM) in control conditions (black squares, n = 104) and in the presence of DTT (10 mM, gray triangles, n = 168). Blocked lines depict the duration of drug treatment.

MitoTracker Orange, we found specific mitochondrial fluorescence in five out of five inside-out patches from nt-HEK cells, five out of five patches from stably transfected hTRPA1-HEK, and three out of three patches from stably transfected hTRPV1-HEK (Fig. 7, F and G, and unpublished data). To confirm that excised-patch mitochondria were responsible for the antimycin A-induced TRPA1 activation, we pretreated the inside-out patch for 4 minutes with a combination of tempol (100 μM), SOD (10 IU/ml), and catalase (100 IU/ml). ROS scavenging by this combination of tempol and enzymes significantly inhibited the antimycin A-induced increase in TRPA1 open probabilities ($n = 4, P < 0.05$). Similar to the Ca^{2+} imaging studies, the scavenging of ROS had no effect on direct activation of TRPA1 by AITC (10 μM, unpublished data).

Discussion

Mitochondrial function is altered in airway inflammatory disease states such as asthma and chronic obstructive pulmonary disease (Rabinovich et al., 2007; Mabalirajan et al., 2008; Aguilera-Aguirre et al., 2009). Given that peripheral sensory nerve terminals are densely packed with mitochondria (Hung et al., 1973; von During and Andres, 1988), we investigated the effect of mitochondrial modulation on sensory nerve function. In the present study we have shown that acute mitochondrial dysfunction selectively activates nociceptive vagal nerves and fails to activate non-nociceptive nerves. Nociceptive nerves protect the innervated organ through the initiation of reflexes and behavioral responses (Carr and Undem, 2003). Thus we present evidence of a novel mechanism by which nocifensive airway responses can be evoked.

We found that 20 μM antimycin A caused action potential discharge in nociceptive bronchopulmonary C-fibers and also activated dissociated vagal nociceptive neurons (as assessed by Ca^{2+} imaging), suggesting that *neuronal* mitochondria were sufficient for the antimycin A-induced responses. The antimycin A-induced increase in $[Ca^{2+}]_i$ was dependent on

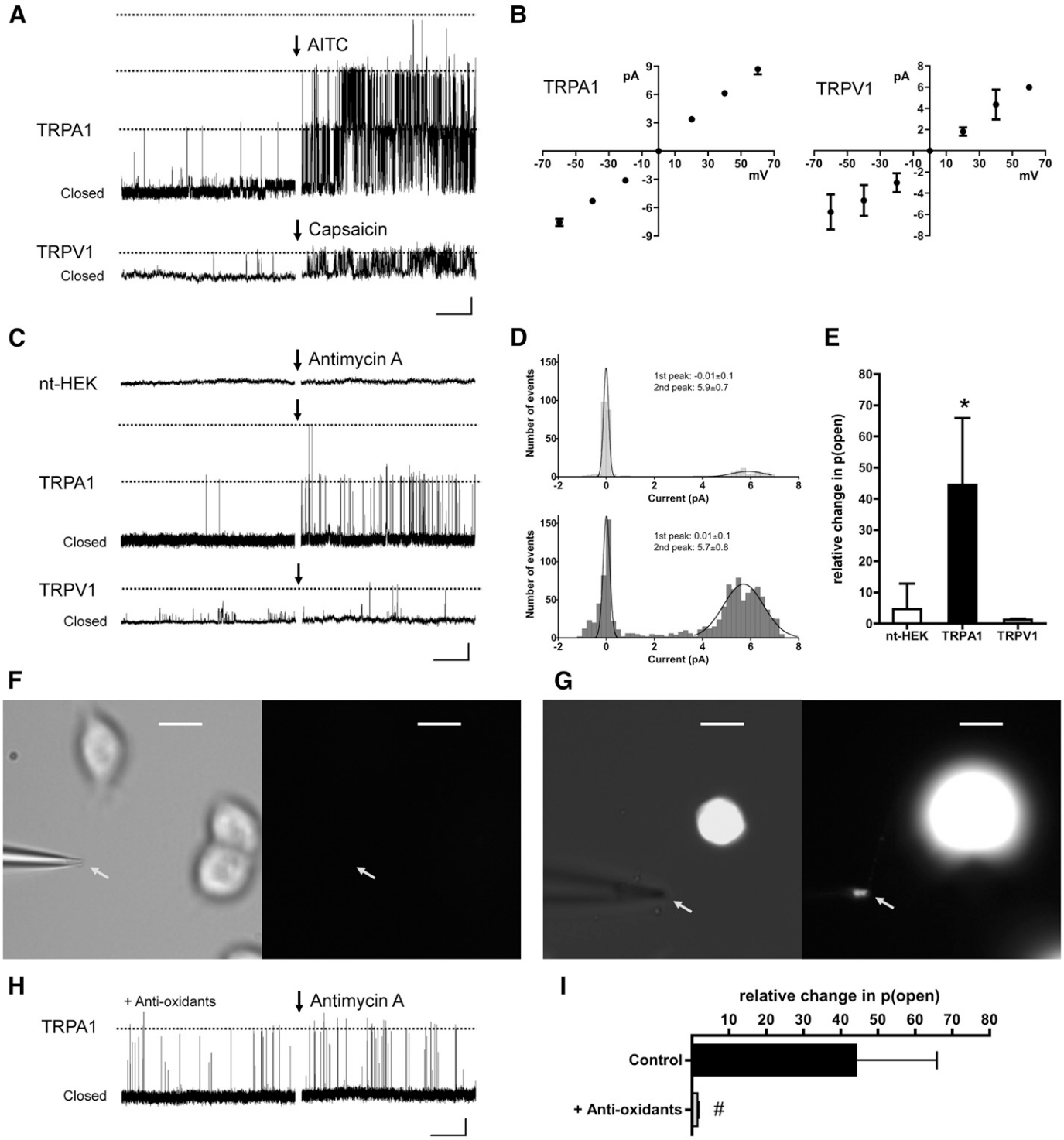

Fig. 7. Antimycin A evokes single-channel TRPA1 currents in inside-out patches due to the presence of mitochondria in excised patches. (A) Representative recordings of single-channel activities in inside-out patches held at +40 mV from HEK cells transiently expressing hTRPA1 (top, three channels) and hTRPV1 (bottom, 1 channel) before and after exposure to AITC (10 μM) or capsaicin (300 nM). Dotted lines indicate currents through a single ion channel. Marker denotes 2 pA and 2 seconds. (B) Mean ± S.E.M. I-V relationship for individual TRPA1 (n = 13, left) and TRPV1 single channel recordings (n = 4, right) derived from 100-ms voltage steps under control conditions. (C) Representative single-channel activities in response to antimycin A (10 μM) in inside-out patches held at +40 mV from nt-HEK cells (top) and HEK cells expressing hTRPA1 (middle, two channels) or hTRPV1 (bottom, 1 channel). Dotted lines indicate currents through a single-ion channel. Marker denotes 2 pA and 2 seconds. (D) Representative current amplitude histograms of an inside-out patch containing a single TRPA1 channel before (top) and after antimycin A (bottom). Data fitted by Gaussian distribution (mean ± S.D. indicated). (E) Mean ± S.E.M. relative change in channel opening probability in response to antimycin A. *Significant increase compared with nt-HEK ($P < 0.05$). (F and G) Representative images of inside-out excised patches from HEK293 cells. Arrow indicates the location of the patch (note that the patch is in focus but in a different focal plane to neighboring cells). Line denotes 15 μm. (F) Inside-out patch from unlabeled nt-HEK cell in brightfield (left) and under rhodamine fluorescence (right). Note the lack of fluorescence in the patch. (G) Rhodamine fluorescence of patch pipette before (left, combination of brightfield and fluorescence images) and after (right, fluorescence image only) inside-out patch excision from nt-HEK cell labeled with MitoTracker Orange (500 ng/ml). Note the presence of mitochondria in the patch. (H) Representative single-channel activities in the

extracellular Ca^{2+}, indicating that plasma membrane ion channels were involved. Bronchopulmonary single nerve fiber recordings showed that nociceptors expressing TRPA1 had significantly greater action potential discharge in response to antimycin A than the nociceptors not expressing TRPA1. Pharmacologic (HC-030031) or genetic blockade of TRPA1 significantly decreased both the action potential discharge in TRPA1-expressing nociceptive bronchopulmonary nerves and the Ca^{2+} influx in vagal neurons, indicating that TRPA1 was the major molecular transduction mechanism for antimycin A-induced nerve activation. The contribution of TRPV1 to antimycin A-induced sensory nerve activation was not as prominent or consistent. The TRPV1 antagonist I-RTX or genetic knockout of TRPV1 caused a minor but significant reduction in antimycin A-induced Ca^{2+} influx in vagal neurons. Indeed, blockade of both TRPA1 and TRPV1 was required to abolish the antimycin A-induced Ca^{2+} influx response. However, in recordings from bronchopulmonary C-fiber nerve terminals, inhibition of TRPV1 only caused significant reductions in the action potential discharge from *fibers that did not express TRPA1*. Thus antimycin A responses are largely mediated by TRPA1, with residual responses due to TRPV1 activation. We have previously shown preferential action potential discharge from bronchopulmonary C-fibers via TRPA1 (as opposed to TRPV1) in response to 4-oxononenal, a product of lipid peroxidation that activates TRPA1 and TRPV1 in Ca^{2+} imaging studies (Taylor-Clark et al., 2008a).

TRP channels are polymodal nonselective cation channels (Patapoutian et al., 2009). TRPV1 and TRPA1 are almost exclusively expressed on nociceptive nerves (Caterina et al., 1997; Jordt et al., 2004). TRPA1 is activated by oxidant/electrophilic compounds derived from plants (Jordt et al., 2004), pollution (Bautista et al., 2006), inflammation and oxidative stress (Trevisani et al., 2007; Andersson et al., 2008; Taylor-Clark et al., 2008a,b), and also by nonelectrophilic compounds such as menthol and cannabinoids (Jordt et al., 2004). TRPV1 is activated by capsaicin, protons, heat, and inflammatory mediators (Caterina et al., 1997; Hwang et al., 2000), and there is evidence to suggest that TRPV1 is also activated by certain electrophilic compounds (Salazar et al., 2008; Taylor-Clark et al., 2008a). Here, consistent with our neuronal data, we found that in heterologous cell systems both TRPA1 and TRPV1 were activated by antimycin A. Antimycin A induced Ca^{2+} influx and evoked outwardly rectifying currents in hTRPA1- and hTRPV1-expressing HEK cells that were blocked by the selective TRPA1 inhibitor HC-030031 and the TRP channel blocker ruthenium red, respectively. Both Ca^{2+} imaging and whole-cell patch data indicated that TRPA1 was more robustly activated following mitochondrial modulation than TRPV1. Antimycin A activated heterologously-expressed TRPA1 between 0.5 μM and 20 μM, consistent with previous reports of superoxide production by antimycin A at these concentrations in intact cells (Li et al., 2003; Kim and Usachev, 2009; Liu et al., 2010; Gonzalez-Dosal et al., 2012). Curve-fitting analysis demonstrated an apparent EC_{50} of ~2 μM with a Hill slope of ~3. It is difficult to place firm conclusions on the biologic significance of this Hill slope value given that the hypothesized mechanism linking antimycin A with TRPA1 activation involves multiple components [i.e., complex III inhibition by antimycin, superoxide production, ROS processing (overcoming catalysis, conversion to other ROS), reaction with multiple cysteines on TRPA1, Ca^{2+} modulation of TRPA1 currents]. In our neuronal preparations, 20-μM antimycin A also produced substantial TRP-dependent vagal neuron activation. However, we did not determine a concentration-response relationship in these studies; thus, we are presently unable to compare mitochondrial dysfunction sensitivity of native neurons to HEK293 cells.

Our mechanistic data in HEK293 cells indicates that antimycin A induces TRPA1 activation indirectly, dependent on the actions of ROS produced by mitochondria. Myxothiazol, an inhibitor of the Q_o site on mitochondrial ETC complex III causes mitochondrial depolarization like antimycin (Q_i site inhibitor), but myxothiazol evokes little superoxide production from complex III and causes almost complete abolition of superoxide production by subsequent antimycin A treatment (Turrens et al., 1985; Gyulkhandanyan and Pennefather, 2004; Tretter et al., 2007). Myxothiazol reduced antimycin A-induced hTRPA1 activation in Ca^{2+} imaging studies, indicating that superoxide production from mitochondria was critical for TRPA1 activation. In some systems the complex I inhibitor rotenone has been shown to reduce antimycin A-induced superoxide production (Stowe and Camara, 2009). However, in intact cells with normal glycolysis/citric acid cycle rotenone can also evoke superoxide production from mitochondria (Li et al., 2003; Gyulkhandanyan and Pennefather, 2004; Stowe and Camara, 2009). We found that rotenone (500 nM) caused selective activation of TRPA1 but also reduced antimycin A-induced TRPA1 activation (unpublished data). Further investigation is required to determine whether antimycin A-induced TRPA1 activation is inhibited by rotenone due to a reduction in evoked ROS or due to desensitization of TRPA1 to ROS.

Superoxide is converted into H_2O_2 by SOD enzymes in both the mitochondria and cytosol. H_2O_2 has been shown to activate TRPA1 directly through DTT-sensitive oxidation of N-terminal cysteines (Andersson et al., 2008; Sawada et al., 2008; Takahashi et al., 2008). Exogenously applied superoxide also activates heterologously expressed TRPA1 channels (Sawada et al., 2008), although it is likely (but not proven) that this occurs indirectly following its conversion to H_2O_2. Our data indicates that the SOD/catalase mimetic MnTMPyP reduced antimycin A-induced TRPA1 activation by approximately 30%, whereas the SOD mimetic tempol had little effect. This suggests that H_2O_2 may play a more prominent role than superoxide in antimycin-induced TRPA1 activation. However, a combination of tempol and MnTMPyP virtually abolished TRPA1 activation by antimycin A. The synergistic

presence of a combination of tempol (100 μM), SOD (10 units/ml), and catalase (100 units/ml) in response to antimycin A (10 μM) from an inside-out patch from a HEK cell expressing hTRPA1 (1 channel). Dotted lines indicate currents through a single-ion channel. Marker denotes 2 pA and 2 seconds. (I) mean ± S.E.M. relative change in TRPA1 channel opening probability in response to antimycin A, without and with antioxidant combination treatment. #Significant decrease compared with control antimycin A responses ($P < 0.05$).

effects of these antioxidant enzyme mimetics in reducing antimycin A-induced responses indicates that both H_2O_2 and superoxide contribute to TRPA1 activation downstream of mitochondrial modulation. Consistent with the Ca^{2+} imaging data in whole cells, a combination of tempol, SOD, and catalase reduced antimycin A-induced TRPA1 channel conductances in excised inside-out patches (that were shown to contain mitochondria using MitoTracker Orange). Nevertheless, it is not yet known if superoxide and H_2O_2 act in series or in parallel to activate TRPA1. DTT, a reducing agent, is able to distinguish between TRPA1 activation by ROS (e.g., H_2O_2) and by α,β-unsaturated carbonyl compounds produced downstream of ROS-mediated lipid peroxidation (e.g., 4-hydoxynonenal) (Andersson et al., 2008; Takahashi et al., 2008): DTT reverses sulfhydryl group oxidation/disulfide bond formation of exposed cysteine residues but cannot reverse sulfhydryl modification by Michael addition reactions (Getz et al., 1999). DTT completely blocked TRPA1 activation following mitochondrial modulation, suggesting that TRPA1 activation was due to ROS (likely H_2O_2) acting directly on the channel. In conclusion, our mechanistic studies indicate that 2 μM antimycin A activated TRPA1 downstream of mitochondrial ROS. We predict that the ROS-dependent mechanism would be critical for TRPA1 activation by other antimycin A concentrations, although there is the possibility that other mechanisms are involved at higher concentrations. Further studies are required to confirm this ROS-dependent mechanism in the TRP-dependent activation of native neurons by mitochondrial dysfunction.

TRPA1 was highly sensitive to mitochondrial modulation by antimycin, to the extent that superoxide production by very limited numbers of mitochondria in excised patches (likely <3, based upon space restrictions) were capable of significant ROS-mediated channel activation within a short time frame (<20 seconds). There remains the minor possibility that there was a direct interaction between antimycin A and TRPA1 in excised patches, although both the sensitivity of antimycin A-induced TRPA1 activation to ROS scavengers and the lack of cysteine-modification by antimycin A argues against this hypothesis. We briefly investigated the possibility that TRPA1 was, in addition to being expressed on the plasma membrane, also expressed in mitochondria. Using a V5-tagged hTRPA1 protein and the mitochondrial-specific fluorescent probe MitoTracker Orange, we found no colocalization of TRPA1 (detected by primary antibody against V5) with MitoTracker Orange following channel overexpression in HEK293 as determined by confocal microscopy (unpublished data), indicating that TRPA1 is not a mitochondrial protein.

Our finding that mitochondrial dysfunction is sufficient to evoke airway sensory nerve activation is likely to be relevant for other sensory nerve types. Mitochondrial dysfunction and subsequent ROS production occurs in diseases such as type II diabetes, irritable bowel syndrome, and cardiovascular disease (Hall and Wiley, 1998; Rocha et al., 2010; Chowdhury et al., 2013). As such, we predict that mitochondrial-TRPA1 interactions may contribute to nociceptor activation in these pathologies. In the airways, mitochondrial dysfunction and oxidative stress has been demonstrated for an array of cell types both in asthma and chronic obstructive bronchitis (Rabinovich et al., 2007; Reddy, 2011) and can be initiated by a wide variety of inflammatory signaling pathways common in respiratory diseases: e.g., tumor necrosis factor α (Corda et al., 2001), neurotrophins via p75NTR (Pehar et al., 2007), microRNAs (Aroor et al., 2012), transforming growth factor β (Michaeloudes et al., 2011), and Toll-like receptors (West et al., 2011). Airway vagal nociceptor activation and hyperexcitability contribute to cough, dyspnea, bronchospasm, and hypersecretion (Carr and Undem, 2003). Given the abundance of mitochondria at the sensory nerve termini and their susceptibility to various inflammatory mediators, we suggest that mitochondrial dysfunction-induced sensory nerve activation represents a novel mechanism by which inflammation is transduced into nociceptive electrical signaling and thus contributes to the symptoms of airway disease. Lastly, our data show that under the present conditions of acute mitochondrial dysfunction vagal bronchopulmonary C-fibers and vagal dissociated neurons respond adequately to further stimulation (mechanical, chemical, and electrical), suggesting that mitochondrial dysfunction (and subsequent oxidative stress) does not necessarily lead to cytotoxicity. Whether chronic mitochondrial dysfunction occurs in airway sensory nerves in inflammatory lung disease is a concept that requires further study.

Acknowledgments

The authors thank Dr. M. A. McAlexander (GlaxoSmithKline) for the kind gift of the stable cell lines and the BacMam virus encoding hTRPA1.

Authorship Contributions

Participated in research design: Nesuashvili, Bahia, Taylor-Clark.

Conducted experiments: Nesuashvili, Hadley, Bahia, Taylor-Clark.

Performed data analysis: Nesuashvili, Hadley, Bahia, Taylor-Clark.

Contributed to the writing of the manuscript: Nesuashvili, Bahia, Taylor-Clark.

References

Aguilera-Aguirre L, Bacsi A, Saavedra-Molina A, Kurosky A, Sur S, and Boldogh I (2009) Mitochondrial dysfunction increases allergic airway inflammation. *J Immunol* **183**:5379–5387.

Andersson DA, Gentry C, Moss S, and Bevan S (2008) Transient receptor potential A1 is a sensory receptor for multiple products of oxidative stress. *J Neurosci* **28**: 2485–2494.

Andrè E, Campi B, Materazzi S, Trevisani M, Amadesi S, Massi D, Creminon C, Vaksman N, Nassini R, and Civelli M et al. (2008) Cigarette smoke-induced neurogenic inflammation is mediated by alpha,beta-unsaturated aldehydes and the TRPA1 receptor in rodents. *J Clin Invest* **118**:2574–2582.

Aroor AR, Mandavia C, Ren J, Sowers JR, and Pulakat L (2012) Mitochondria and oxidative stress in the cardiorenal metabolic syndrome. *Cardiorenal Med* **2**:87–109.

Bautista DM, Jordt SE, Nikai T, Tsuruda PR, Read AJ, Poblete J, Yamoah EN, Basbaum AI, and Julius D (2006) TRPA1 mediates the inflammatory actions of environmental irritants and proalgesic agents. *Cell* **124**:1269–1282.

Carr MJ and Undem BJ (2003) Bronchopulmonary afferent nerves. *Respirology* **8**: 291–301.

Caterina MJ, Schumacher MA, Tominaga M, Rosen TA, Levine JD, and Julius D (1997) The capsaicin receptor: a heat-activated ion channel in the pain pathway. *Nature* **389**:816–824.

Chen J and Armstrong RN (1995) Stereoselective catalysis of a retro-Michael reaction by class mu glutathione transferases. Consequences for the internal distribution of products in the active site. *Chem Res Toxicol* **8**:580–585.

Chowdhury SK, Smith DR, and Fernyhough P (2013) The role of aberrant mitochondrial bioenergetics in diabetic neuropathy. *Neurobiol Dis* 51:56–65.

Chuang HH and Lin S (2009) Oxidative challenges sensitize the capsaicin receptor by covalent cysteine modification. *Proc Natl Acad Sci USA* **106**:20097–20102.

Copeland WC (2008) Inherited mitochondrial diseases of DNA replication. *Annu Rev Med* **59**:131–146.

Corda S, Laplace C, Vicaut E, and Duranteau J (2001) Rapid reactive oxygen species production by mitochondria in endothelial cells exposed to tumor necrosis factor-alpha is mediated by ceramide. *Am J Respir Cell Mol Biol* **24**:762–768.

Day BJ, Fridovich I, and Crapo JD (1997) Manganic porphyrins possess catalase activity and protect endothelial cells against hydrogen peroxide-mediated injury. *Arch Biochem Biophys* **347**:256–262.

Faulkner KM, Liochev SI, and Fridovich I (1994) Stable Mn(III) porphyrins mimic superoxide dismutase in vitro and substitute for it in vivo. *J Biol Chem* **269**: 23471–23476.

Forsberg K, Karlsson JA, Theodorsson E, Lundberg JM, and Persson CG (1988) Cough and bronchoconstriction mediated by capsaicin-sensitive sensory neurons in the guinea-pig. *Pulm Pharmacol* **1**:33–39.
Getz EB, Xiao M, Chakrabarty T, Cooke R, and Selvin PR (1999) A comparison between the sulfhydryl reductants tris(2-carboxyethyl)phosphine and dithiothreitol for use in protein biochemistry. *Anal Biochem* **273**:73–80.
Gonzalez-Dosal R, Horan KA, and Paludan SR (2012) Mitochondria-derived reactive oxygen species negatively regulates immune innate signaling pathways triggered by a DNA virus, but not by an RNA virus. *Biochem Biophys Res Commun* **418**: 806–810.
Gyulkhandanyan AV and Pennefather PS (2004) Shift in the localization of sites of hydrogen peroxide production in brain mitochondria by mitochondrial stress. *J Neurochem* **90**:405–421.
Hall KE and Wiley JW (1998) Neural injury, repair and adaptation in the GI tract. I. New insights into neuronal injury: a cautionary tale. *Am J Physiol* **274**: G978–G983.
Hinman A, Chuang HH, Bautista DM, and Julius D (2006) TRP channel activation by reversible covalent modification. *Proc Natl Acad Sci USA* **103**:19564–19568.
Hung KS, Hertweck MS, Hardy JD, and Loosli CG (1973) Ultrastructure of nerves and associated cells in bronchiolar epithelium of the mouse lung. *J Ultrastruct Res* **43**:426–437.
Hwang SW, Cho H, Kwak J, Lee SY, Kang CJ, Jung J, Cho S, Min KH, Suh YG, and Kim D et al. (2000) Direct activation of capsaicin receptors by products of lipoxygenases: endogenous capsaicin-like substances. *Proc Natl Acad Sci USA* **97**: 6155–6160.
Jordt SE, Bautista DM, Chuang HH, McKemy DD, Zygmunt PM, Högestätt ED, Meng ID, and Julius D (2004) Mustard oils and cannabinoids excite sensory nerve fibres through the TRP channel ANKTM1. *Nature* **427**:260–265.
Karihtala P and Soini Y (2007) Reactive oxygen species and antioxidant mechanisms in human tissues and their relation to malignancies. *APMIS* **115**:81–103.
Kim D and Cavanaugh EJ (2007) Requirement of a soluble intracellular factor for activation of transient receptor potential A1 by pungent chemicals: role of inorganic polyphosphates. *J Neurosci* **27**:6500–6509.
Kim MS and Usachev YM (2009) Mitochondrial Ca2+ cycling facilitates activation of the transcription factor NFAT in sensory neurons. *J Neurosci* **29**:12101–12114.
Kollarik M, Dinh QT, Fischer A, and Undem BJ (2003) Capsaicin-sensitive and -insensitive vagal bronchopulmonary C-fibres in the mouse. *J Physiol* **551**:869–879.
Krishna MC, Russo A, Mitchell JB, Goldstein S, Dafni H, and Samuni A (1996) Do nitroxide antioxidants act as scavengers of O2-. or as SOD mimics? *J Biol Chem* **271**:26026–26031.
Li N, Ragheb K, Lawler G, Sturgis J, Rajwa B, Melendez JA, and Robinson JP (2003) Mitochondrial complex I inhibitor rotenone induces apoptosis through enhancing mitochondrial reactive oxygen species production. *J Biol Chem* **278**:8516–8525.
Liu M, Liu H, and Dudley SC, Jr (2010) Reactive oxygen species originating from mitochondria regulate the cardiac sodium channel. *Circ Res* **107**:967–974.
Mabalirajan U, Dinda AK, Kumar S, Roshan R, Gupta P, Sharma SK, and Ghosh B (2008) Mitochondrial structural changes and dysfunction are associated with experimental allergic asthma. *J Immunol* **181**:3540–3548.
Macpherson LJ, Dubin AE, Evans MJ, Marr F, Schultz PG, Cravatt BF, and Patapoutian A (2007) Noxious compounds activate TRPA1 ion channels through covalent modification of cysteines. *Nature* **445**:541–545.
McNamara CR, Mandel-Brehm J, Bautista DM, Siemens J, Deranian KL, Zhao M, Hayward NJ, Chong JA, Julius D, and Moran MM et al. (2007) TRPA1 mediates formalin-induced pain. *Proc Natl Acad Sci USA* **104**:13525–13530.
Michaeloudes C, Sukkar MB, Khorasani NM, Bhavsar PK, and Chung KF (2011) TGF-{beta} regulates Nox4, MnSOD and catalase expression and IL-6 release in airway smooth muscle cells. *Am J Physiol Lung Cell Mol Physiol* **300**: L295–L304.
Nassenstein C, Kwong K, Taylor-Clark T, Kollarik M, Macglashan DM, Braun A, and Undem BJ (2008) Expression and function of the ion channel TRPA1 in vagal afferent nerves innervating mouse lungs. *J Physiol* **586**:1595–1604.
Patapoutian A, Tate S, and Woolf CJ (2009) Transient receptor potential channels: targeting pain at the source. *Nat Rev Drug Discov* **8**:55–68.
Pehar M, Vargas MR, Robinson KM, Cassina P, Díaz-Amarilla PJ, Hagen TM, Radi R, Barbeito L, and Beckman JS (2007) Mitochondrial superoxide production and nuclear factor erythroid 2-related factor 2 activation in p75 neurotrophin receptor-induced motor neuron apoptosis. *J Neurosci* **27**:7777–7785.
Potter VR and Reif AE (1952) Inhibition of an electron transport component by antimycin A. *J Biol Chem* **194**:287–297.
Rabinovich RA, Bastos R, Ardite E, Llinàs L, Orozco-Levi M, Gea J, Vilaró J, Barberà JA, Rodríguez-Roisin R, and Fernández-Checa JC et al. (2007) Mitochondrial dysfunction in COPD patients with low body mass index. *Eur Respir J* **29**:643–650.
Reddy PH (2011) Mitochondrial dysfunction and oxidative stress in asthma: implications for mitochondria-targeted antioxidant therapeutics. *Pharmaceuticals* **4**:429–456.
Rocha M, Apostolova N, Hernandez-Mijares A, Herance R, and Victor VM (2010) Oxidative stress and endothelial dysfunction in cardiovascular disease: mitochondria-targeted therapeutics. *Curr Med Chem* **17**:3827–3841.
Rustenbeck I, Dickel C, Herrmann C, and Grimmsmann T (1999) Mitochondria present in excised patches from pancreatic B-cells may form microcompartments with ATP-dependent potassium channels. *Biosci Rep* **19**:89–98.
Salazar H, Llorente I, Jara-Oseguera A, García-Villegas R, Munari M, Gordon SE, Islas LD, and Rosenbaum T (2008) A single N-terminal cysteine in TRPV1 determines activation by pungent compounds from onion and garlic. *Nat Neurosci* **11**:255–261.
Sawada Y, Hosokawa H, Matsumura K, and Kobayashi S (2008) Activation of transient receptor potential ankyrin 1 by hydrogen peroxide. *Eur J Neurosci* **27**:1131–1142.
Slater EC (1973) The mechanism of action of the respiratory inhibitor, antimycin. *Biochim Biophys Acta* **301**:129–154.
Story GM, Peier AM, Reeve AJ, Eid SR, Mosbacher J, Hricik TR, Earley TJ, Hergarden AC, Andersson DA, and Hwang SW et al. (2003) ANKTM1, a TRP-like channel expressed in nociceptive neurons, is activated by cold temperatures. *Cell* **112**:819–829.
Stowe DF and Camara AK (2009) Mitochondrial reactive oxygen species production in excitable cells: modulators of mitochondrial and cell function. *Antioxid Redox Signal* **11**:1373–1414.
Susankova K, Tousova K, Vyklicky L, Teisinger J, and Vlachova V (2006) Reducing and oxidizing agents sensitize heat-activated vanilloid receptor (TRPV1) current. *Mol Pharmacol* **70**:383–394.
Takahashi N, Mizuno Y, Kozai D, Yamamoto S, Kiyonaka S, Shibata T, Uchida K, and Mori Y (2008) Molecular characterization of TRPA1 channel activation by cysteine-reactive inflammatory mediators. *Channels (Austin)* **2**:287–298.
Taylor-Clark TE, McAlexander MA, Nassenstein C, Sheardown SA, Wilson S, Thornton J, Carr MJ, and Undem BJ (2008a) Relative contributions of TRPA1 and TRPV1 channels in the activation of vagal bronchopulmonary C-fibres by the endogenous autacoid 4-oxononenal. *J Physiol* **586**:3447–3459.
Taylor-Clark TE, Undem BJ, Macglashan DW, Jr, Ghatta S, Carr MJ, and McAlexander MA (2008b) Prostaglandin-induced activation of nociceptive neurons via direct interaction with transient receptor potential A1 (TRPA1). *Mol Pharmacol* **73**:274–281.
Taylor-Clark TE, Ghatta S, Bettner W, and Undem BJ (2009) Nitrooleic acid, an endogenous product of nitrative stress, activates nociceptive sensory nerves via the direct activation of TRPA1. *Mol Pharmacol* **75**:820–829.
Tretter L, Takacs K, Hegedus V, and Adam-Vizi V (2007) Characteristics of alpha-glycerophosphate-evoked H2O2 generation in brain mitochondria. *J Neurochem* **100**:650–663.
Trevisani M, Siemens J, Materazzi S, Bautista DM, Nassini R, Campi B, Imamachi N, Andrè E, Patacchini R, and Cottrell GS et al. (2007) 4-Hydroxynonenal, an endogenous aldehyde, causes pain and neurogenic inflammation through activation of the irritant receptor TRPA1. *Proc Natl Acad Sci USA* **104**:13519–13524.
Turrens JF, Alexandre A, and Lehninger AL (1985) Ubisemiquinone is the electron donor for superoxide formation by complex III of heart mitochondria. *Arch Biochem Biophys* **237**:408–414.
Undem BJ, Chuaychoo B, Lee MG, Weinreich D, Myers AC, and Kollarik M (2004) Subtypes of vagal afferent C-fibres in guinea-pig lungs. *J Physiol* **556**:905–917.
von Düring M and Andres KH (1988) Structure and functional anatomy of visceroreceptors in the mammalian respiratory system. *Prog Brain Res* **74**:139–154.
Wahl P, Foged C, Tullin S, and Thomsen C (2001) Iodo-resiniferatoxin, a new potent vanilloid receptor antagonist. *Mol Pharmacol* **59**:9–15.
West AP, Brodsky IE, Rahner C, Woo DK, Erdjument-Bromage H, Tempst P, Walsh MC, Choi Y, Shadel GS, and Ghosh S (2011) TLR signalling augments macrophage bactericidal activity through mitochondrial ROS. *Nature* **472**:476–480.
Zurborg S, Yurgionas B, Jira JA, Caspani O and Heppenstall PA (2007) Direct activation of the ion channel TRPA1 by Ca(2+). *Nat Neurosci* 10:277–279.

Address correspondence to: Dr. Thomas Taylor-Clark, 12901 Bruce B. Downs Blvd, University of South Florida, Tampa, FL 33612. ttaylorc@health.usf.edu